The Use of pHluorins for Optical Measurements of Presynaptic Activity

Sethuraman Sankaranarayanan,* Dino De Angelis,† James E. Rothman,† and Timothy A. Ryan*
*Department of Biochemistry, The Weill Medical College of Cornell University and †Sloan-Kettering Institute, Memorial Sloan-Kettering Cancer Center, New York, New York 10021 USA

ABSTRACT Genetically encoded reporters for optical measurements of presynaptic activity hold significant promise for measurements of neurotransmission within intact or semi-intact neuronal networks. We have characterized pH-sensitive green fluorescent protein-based sensors (pHluorins) of synaptic vesicle cycling at nerve terminals. pHluorins have a pK ~ 7.1, which make them ideal for tracking synaptic vesicle lumen pH upon cycling through the plasma membrane during action potentials. A theoretical analysis of the expected signals using this approach and guidelines for future reporter development are provided.

INTRODUCTION

Chemical synaptic transmission between neurons is a major means of communication mediating information flow in the brain. Monitoring of synaptic events during behavioral or cognitive tasks would ultimately provide important understanding of the link between collective neuronal network function and the demands placed upon cellular machinery. Clear interpretations of electrically recorded synaptic events in intact or semi-intact neuronal networks are, however, hampered by several problems. First, the complexity of the neural circuit is such that responses from single synaptic sites are often hard to extract, and second, electrical filtering properties of the dendrites strongly shape synaptic responses recorded in the postsynaptic neuron. In addition, postsynaptic electrical recordings usually obscure many of the underlying cell biological and molecular events that support presynaptic function. The advent of new optical recording techniques (Denk and Svoboda, 1997; Helmchen et al., 1999) in combination with advances in fluorescent molecular probes (Tsien, 1998; Matz et al., 1999) together are poised to provide new levels of information about the functioning of multicellular neuronal networks and the underlying cellular and molecular machinery that govern their behavior. Recently, a novel approach that uses pH-sensitive green fluorescent protein (GFP) has been applied to visualize secretion at synaptic terminals (Miesenböck et al., 1998). Because this is a genetically encoded reporter, it holds significant promise for future studies in a number of genetic systems, including drosophila, nematode, zebrafish, and mouse.

The functional basis of pH-based sensors of synaptic activity is diagrammed in Fig. 1. Synaptic vesicles are specialized endosomes that maintain an acidic lumen resulting from the activity of a vacuolar H^+ ATPase (Nelson, 1992). This activity is required to establish an electromotive force that, in turn, drives neurotransmitter uptake from the cytosol into the vesicle (Liu et al., 1999). Measurements of synaptic vesicle lumen pH indicate that it has a resting value of ~5.6 (Miesenböck et al., 1998). Following fusion with the plasma membrane during action potential firing, the lumenal surface of the synaptic vesicle abruptly switches to the more alkaline pH of the extracellular environment (pH ~ 7.4). A histidine-based combinatorial mutagenesis strategy combined with a pH-dependent selection screen was used by Miesenböck and coworkers to obtain new variants of GFP that enable measurements of synaptic vesicle exocytosis. These new GFPs were termed pH-sensitive green fluorescent protein-based sensors (pHluorins). pHluorins targeted to the synaptic vesicle lumen (synapto-pHluorin) enabled measurements of dynamic changes in pH of vesicle lumen resulting from exocytosis and endocytosis of synaptic vesicles during presynaptic activity. The net fluorescence change observed during action potentials therefore reflect a net balance of externalized pHluorin, which is brightly fluorescent, and the endocytosed and reacidified vesicles, which are dark. Here we have characterized the use of pHluorins for measuring exocytosis at synaptic terminals, determined their pK, and provide an analytical framework for understanding the magnitude of the optical signals generated by fusion of synaptic vesicles with the plasma membrane.

METHODS

Cell preparation and transfection

Hippocampal CA1–CA3 regions were dissected from 4-day-old Sprague-Dawley rats, dissociated, prepared, and plated onto polyornithine-coated glass coverslips as previously described (Ryan 1999). Coverslips were mounted in a rapid switching, laminar-flow perfusion and stimulation chamber on the stage of a custom-built laser-scanning confocal microscope. The total volume of the chamber was ~75 μl and was perfused at a rate of 1–1.5 ml/min. Action potentials were evoked by passing 1-ms current pulses, yielding fields of ~10 V/cm, through the chamber via Platinum-Iridium electrodes. Except as otherwise noted, cells were continuously perfused at room temperature (~24°C) in a standard saline solution containing in mM: 119 NaCl, 2.5 KCl, 2 $CaCl_2$, 2 $MgCl_2$, 25 HEPES (buffered to pH 7.4), 30 glucose, 10 μM 6-cyano-7-nitroquinoxaline-2,3-

Received for publication 3 April 2000 and in final form 28 June 2000.

Address reprint requests to Timothy A. Ryan, Ph.D., Department of Biochemistry, Room E-107, Weill Medical College of Cornell University, 1300 York Ave., New York, NY 10021. Tel: 212-746-6403; Fax: 212-746-8875; E-mail: taryan@mail.med.cornell.edu.

0006-3495/00/10/2199/10 $2.00

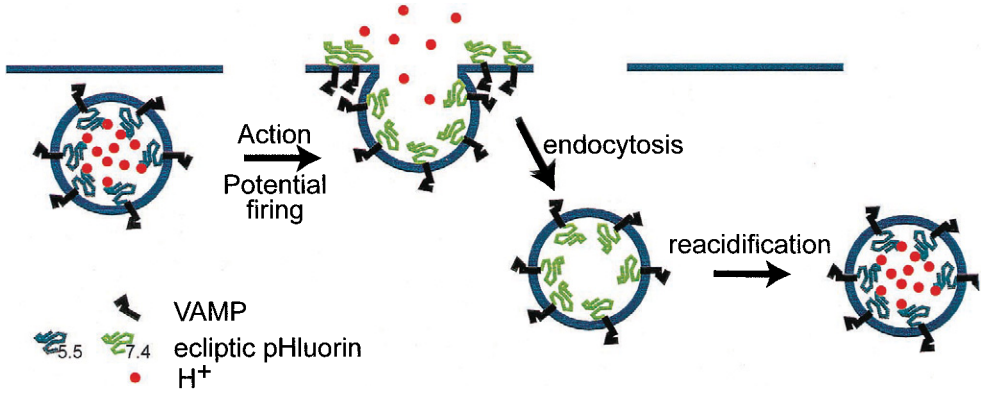

FIGURE 1 Exocytosis relieves the proton-dependent quenching of ecliptic-pHluorin fluorescence. The pHluorin molecule is attached to the lumenal aspect of VAMP. At the resting pH of 5.6 within vesicles, the fluorescence signal from pHluorin is completely quenched. During firing of action potentials, the vesicles undergo fusion with the plasma membrane leading to the externalization of pHluorin to pH of 7.4. This relieves the proton-dependent quenching and causes an increase in fluorescence. The fluorescence signal then recovers following endocytosis by reacidification of vesicles.

dione, and 50 μM D,L-2-amino-5-phosphonovaleric acid. Ammonium chloride solution (pH 7.4) was prepared by substituting 50 mM NaCl in the above saline with NH_4Cl, all other components remaining unchanged. Alkaline solutions with final pH of 8.5 and 9.5 were prepared by replacing HEPES in the standard saline with Bicine (pK_a = 8.3). Acidic-solutions with final pH of 3.5 (nominally pH-adjusted), 4.5 and 5.5 were prepared by replacing HEPES in the standard saline with MES (pK_a = 6.1), all other components in the saline remaining unchanged.

Calcium phosphate-mediated gene transfer (Threadgill et al., 1997) was used to transfect 6–8-day-old cultures with ecliptic or enhanced ecliptic (superecliptic) synapto-pHluorin in a pCI vector (Promega, Madison, WI) (Miesenböck et al., 1998). The superecliptic variant contains two mutations (F64L and S65T) in the original ecliptic pHluorin probe leading to enhanced fluorescence. Briefly, cultures were washed once with MEM and incubated for 1 hr at 37°C. The DNA/$CaPO_4$ precipitate was prepared by gently vortexing a mixture of $CaCl_2$ 2M (20×), plasmid DNA (final concentration ~0.1 μg/μl), and 2 × HEPES-buffered saline (in gm/liter: 16 NaCl, 0.7 KCl, 0.4 Na_2HPO_4, 2.7 Glucose, 10 HEPES, pH ~7.1) and allowed to sit in the dark for 15 min. The precipitate was overlaid on the cells, allowed to incubate for 20 min at 37°C. Cells were then washed twice with MEM, re-fed with culture medium, and replaced in the incubator. All experiments were performed between 4 and 12 days after transfection. (The ecliptic and superecliptic constructs were generated by D.D. and J.E.R. whereas S.S. and T.A.R. performed all experiments and analysis reported in this manuscript.)

Optical measurements, microscopy and analysis

Laser-scanning fluorescence and differential interference contrast images were acquired simultaneously using a custom-built laser-scanning microscope. Specimens were illuminated with ~45 μW of the 488-nm line of an argon ion laser that was rapidly shuttered during all nondata-acquiring periods using electro-optic modulation. Time course of fluorescence response of synapto-pHluorin was measured from time-lapse images during action potential firing. Synapto-pHluorin fluorescence emission was collected using a 500–600-nm band-pass filter. Quantitative measurements of fluorescence intensity at individual boutons and neighboring axonal regions were obtained by averaging 4 × 4 square areas of pixel intensities. Individual regions were selected by hand, and the optical center of mass used to center the measurement box was computed over a slightly larger area (typically 8 × 8 pixels). All error bars shown are SEM.

RESULTS

Theoretical basis for pH-based optical signals

Two types of pHluorins were originally isolated, a ratiometric and an ecliptic form (Miesenböck et al., 1998). The fluorescence of the latter is completely quenched at low pH values when excited at 488 nm. Recently, the fluorescence of different forms of GFP, including EGFP, was shown to be pH sensitive (Kneen et al., 1998). Fluorescence-correlation spectroscopy measurements of EGFP in solution (Haupts el al., 1998) indicated that protonation of the hydroxyl group at Tyr-66 quenches the absorption of 488-nm light, and therefore emission at 510 nm vanishes. Thus the protonation reaction provides an all or none fluorescence switch. This switching behavior indicates that, for both EGFP and ecliptic pHluorin (hereafter referred to as e-pHluorin), the magnitude of the fluorescence signal derived from changing the pH will depend upon the fractional change in the number of EGFP or e-pHluorin molecules in the deprotonated state. If one assumes that protonation at a single site is sufficient to quench fluorescence, one can estimate the fluorescence as a function of pH as follows. At any given pH, EGFP or e-pHluorin will be in equilibrium with free protons, so the baseline fluorescence from the vesicles will be set by the Henderson–Hasselbach equation, where the fraction of molecules in the deprotonated state [X] is given by

$$[X] = \frac{1}{(1 + 10^{(pK - pH)})}, \quad (1)$$

where pK is the logarithm of the equilibrium constant for protonation.

For each synaptic vesicle, the predicted change in the fraction of deprotonated EGFP or e-pHluorin molecules

upon fusion with the plasma membrane (i.e., during a pH change from 5.6 to 7.4) will be

$$\Delta[X] = \frac{1}{(1 + 10^{pK-7.4})} - \frac{1}{(1 + 10^{pK-5.6})}. \quad (2)$$

Thus the value of the pK determines the magnitude of this signal. The relative change in the signal for each vesicle upon exocytosis is $\alpha = \Delta[X]/[X]_0$, where $[X]_0$ is the fluorescence at pH 5.6. α is given by the expression

$$\alpha = \frac{\Delta[X]}{[X]_0} = \frac{(1/(1 + 10^{pK-7.4}) - 1/(1 + 10^{pK-5.6}))}{1/(1 + 10^{pK-5.6})}. \quad (3)$$

The pK of EGFP has recently been measured to be ~6.0 (6.0 by Kneen et al., 1998, 5.8 by Haupts et al., 1998), and thus the relative change (α) in the number of deprotonated EGFP molecules per vesicle during exocytosis is predicted to be ~2. Because synaptic terminals in these neurons typically have ~100 or more vesicles (Schikorski and Stevens, 1997), the expected change of fluorescence per synapse for each fusion event will be only ~1 part in 100. Thus, a critical parameter that determines the usefulness of pH-based sensors of vesicle fusion will be the pK of fluorescence quenching.

Measurement of the pK of ecliptic synapto-pHluorin

We had earlier documented that, in hippocampal neurons transfected with e-pHluorin fused to the lumenal domain of vesicle associated membrane protein (VAMP) (referred to as synapto-pHluorin), a small fraction of VAMP is observed on the surface of axons and presynaptic terminals (Sankaranarayanan and Ryan, 2000). To determine whether e-pHluorins would serve as an efficient probe for measuring presynaptic activity, we have used the surface fraction of e-pHluorin to characterize the pH-dependence of its fluorescence properties.

We characterized EGFP and two forms of e-pHluorin, the original form and a variant with enhanced fluorescence properties (superecliptic, referred to as e-pHluorin$_s$). In vitro e-pHluorin$_s$ has ~9 times greater fluorescence yield per molecule compared with the original ecliptic variant (D. De Angelis and J. E. Rothman, unpublished observations). When transiently expressed in hippocampal neurons grown in culture, synapto-pHluorins appear in both presynaptic varicosities and in the intervening axonal regions (Fig. 2 *A*). Previous studies have shown that these varicosities colocalize with synaptic markers (Miesenböck et al., 1998; Sankaranarayanan and Ryan, 2000*)*. On electrical stimulation, an increase in fluorescence is observed at synaptic varicosities and intervening axonal regions (Fig. 2 *A2*) as compared to that at rest (Fig. 2 *A1*) (see Sankaranarayanan and Ryan, 2000). We interpret these to be due to the externalization and deprotonation of vesicle-associated e-pHluorin causing a rise in fluorescence. The presence of a small amount of synapto-pHluorin on the axonal and synaptic surfaces at rest allowed us to determine the equilibrium constant for proton-dependent fluorescence quenching of this probe. Figure 2 *B* shows the time course of fluorescence averaged over 28 synaptic regions during rapid superfusion with buffers titrated to different pH values. The fluorescence intensity was modulated by change in extracellular pH, and, in all cases, the pH-dependent intensity changes were reversible. Superfusion with low pH (5.5) caused a rapid and substantial loss of fluorescence, whereas superfusion with pH 8.5 caused a rapid increase in fluorescence intensity. The fluorescence does not completely vanish, because, even at pH 5.6, roughly 2.5% of the pHluorin molecules exist in the deprotonated state (assuming a pK of 7.1, see below). Similar fluorescence responses were observed in axonal regions (data not shown). Control experiments with cytosolic pH-sensitive dyes indicate that intracellular pH changes during these brief extracellular ΔpH challenges were minimal (data not shown). We surmise that the fluorescence change ΔF in response to a change in pH reflects a change in the fraction of deprotonated molecules. Figure 2 *C* shows a fit of the magnitude of normalized ΔF ($\Delta F/\Delta F_{max}$) as a function of pH to a simple Henderson–Hasselbach equation. These data show that both e-pHluorins had a pK for protonation of ~7.1 (Ecliptic pHluorin: 7.2 ± 0.09, $n = 3$ experiments; Superecliptic: 7.11 ± 0.02, $n = 4$ separate experiments), whereas EGFP had a pK of ~6.0 (6.03 ± 0.04, from 2 separate experiments). Our estimates of pK for EGFP using surface-distributed VAMP-EGFP was similar to that obtained from purified EGFP in solution (Haupts et al., 1998, pK = 5.8; Kneen et al., 1998, pK = 6.0). This close similarity in pK values validates our pH calibration approach using surface-expressed pHluorins.

Using pK = 7.1 in Eq. 3, we estimate that the fluorescence of each synaptic vesicle will increase by $\alpha = 20.7$ upon fusion with the plasma membrane and equilibration to pH 7.4. This is an ~10-fold predicted improvement in signal compared with EGFP.

Surface to total vesicle pool ratio

We designed experiments to determine the relative amount of synapto-pHluorin on the synaptic surface compared to that within acidic organelles (synaptic vesicles) in the synaptic terminal. In addition to modulating the surface fluorescence using low pH quenching, we have used ammonium chloride (NH_4Cl) superfusion to alkalize synaptic vesicles within the terminal. Ammonia, in equilibrium with ammonium ions in solution, diffuses across cell membranes and elevates cytosolic and organelle pH (Roos and Boron, 1981). For the conditions used here, the lumen of synaptic vesicles has been shown to alkalinize to pH ~7.4 upon brief exposure to 50 mM NH_4Cl (Miesenböck et al., 1998). A general expression for determining the surface-to-vesicle

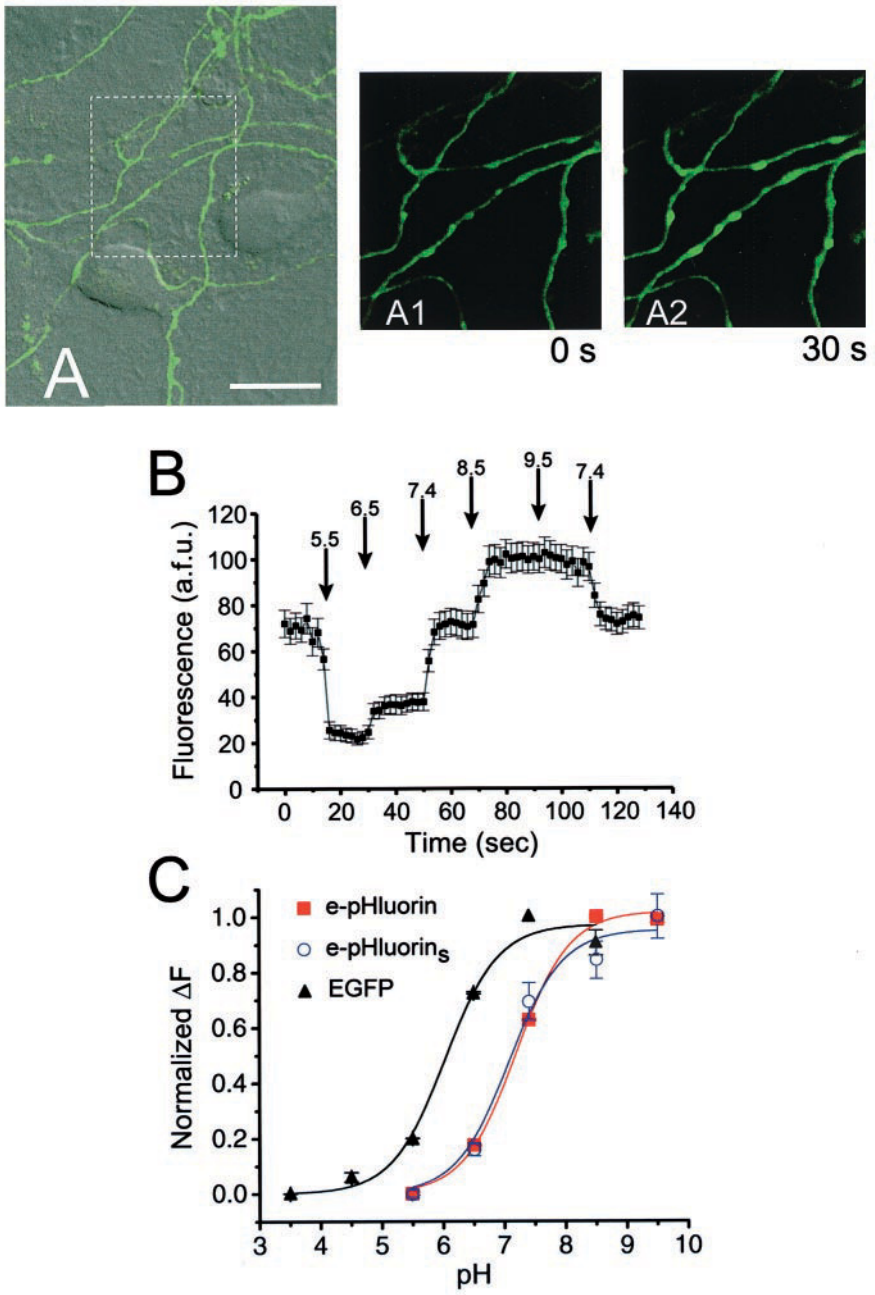

FIGURE 2 Fluorescence signals from pHluorins show a strong pH dependence with an estimated pK of ~7.1. (*A*) DIC-fluorescence overlay of a region of hippocampal neuronal culture eight days after transfection with synapto-pHluorin. The central region of neurites (*dashed box*) is shown at a higher magnification (*A1*) at rest and (*A2*) 30 s after 600 action potential stimulus at 20 Hz. All fluorescence images are shown in false green. The scale bar is 15 μm. (*B*) pHluorins display a strong pH dependence to their fluorescence signals. The average fluorescence time course ($n = 28$ boutons) during a series of pH challenges is illustrated (*downward arrows*). The numbers indicate the respective pH washes. (*C*) The average normalized change in fluorescence (ΔF) from multiple experiments (each experiment contributed 20–40 boutons) is plotted as a function of pH. The number of experiments used in the averaged data was: EGFP ($n = 2$); ecliptic pHluorin ($n = 3$); superecliptic pHluorin ($n = 4$). The respective colored solid lines are fits to the equation $y = y_0 + y_{max}/(1 + 10^{(pK-pH)})$, where y_0 represents the offset, y_{max} the dynamic range, and pK is the logarithm of equilibrium constant for protonation. The pK from the fits were: EGFP = 6.03; ecliptic-pHluorin = 7.07; superecliptic pHluorin = 7.18. The result of fitting similar curves to individual experiments is given in the text.

pool ratio of synapto-pHluorin is derived as follows. The total fluorescence signal (F_{total}) at rest at a given bouton is given by

$$F_{total} = F_{surface} + F_{vesicular}, \quad (4)$$

the sum of the contributions from the surface molecules ($F_{surface}$) and those in acidic vesicles ($F_{vesicular}$). Because the chromophores in the vesicle lumen are at pH 5.6, they will contribute α-fold (α defined in Eq. 3) lower fluorescence on a per molecule basis compared to molecules on the cell surface at pH 7.4.

A general expression is obtained by rewriting Eq. 4 in terms of synapto-pHluorin concentration ([spH]), where β is the amount of fluorescence detected per deprotonated molecule

$$F_0 = ([spH]_s + [spH]_v/(\alpha + 1)) * \beta. \quad (5)$$

During NH_4Cl application, the new fluorescence is

$$F_{NH_4Cl} = ([spH]_s + [spH]_v) * \beta. \quad (6)$$

If one defines the fractional increase during NH_4Cl challenges $\gamma = (F_{NH_4Cl} - F_0)/F_0$, a simple equation can be

derived that relates the fraction of total molecules on the surface of a given bouton (Surface/Total) to the measured quantity γ and the previously determined relative fluorescence increase per vesicle upon exocytosis, α, as

$$f = \left(\frac{\text{Surface}}{\text{Total}}\right) = \frac{\alpha - \gamma}{\alpha\gamma + \alpha}. \quad (7)$$

The average fluorescence response from 26 individual boutons during an NH_4Cl challenge is depicted in Fig. 3 *A*. These data show that the baseline fluorescence increases ~5-fold during this treatment. The magnitude of the NH_4Cl response varies across boutons. We interpret this variation as arising from differences in the surface-to-total ratio at each bouton. Fig. 3 *B* shows the distribution of predicted values of the fractional surface expression across the same population of boutons shown in Fig. 3 *A* derived from Eq. 7. These data indicate that the average fractional expression of synapto-pHluorin on the surface of synaptic terminals is 0.12 ± 0.01, and the median fractional surface expression is 0.11. An expression similar to Eq. 7 to estimate the surface fraction can also be derived from acid-quenching experiments. If one defines the quantity $\epsilon = (F_0 - F_{5.5})/F_0$ as the change in fluorescence observed during a brief acid wash to pH 5.5, by a similar logic to Eqs. 4–6, one can easily derive an alternate expression for f as

$$f = \frac{\varepsilon}{1 - \phi + \alpha(1 - \varepsilon)}, \quad (8)$$

where ϕ is the ratio of fluorescence of pHluorin at pH 5.5 compared to that at pH 5.6. Inspection of the acid-quenching data presented in Fig. 2 *B* shows that the average value of $\epsilon = 0.67$. This yields an average value of $f = 0.10 \pm 0.01$. It is important to note that this approach does not rely upon responses to NH_4Cl, but only the pK and the resting value of synaptic vesicle pH. The good agreement between the acid-quenching and the NH_4Cl methods supports our conclusion that the surface expression of synapto-pHluorin is in the range of 10–15% (see below).

The surface expression of pHluorin that we observed might result from over-expression of exogenous VAMP. To test whether the degree of surface expression and the total amount of synapto-pHluorin expressed in synaptic boutons was correlated, we compared the surface fraction from numerous different experiments with the total synapto-pHluorin content, measured by alkalizing intracellular compartments with ammonium chloride. Figure 3 *C* shows the

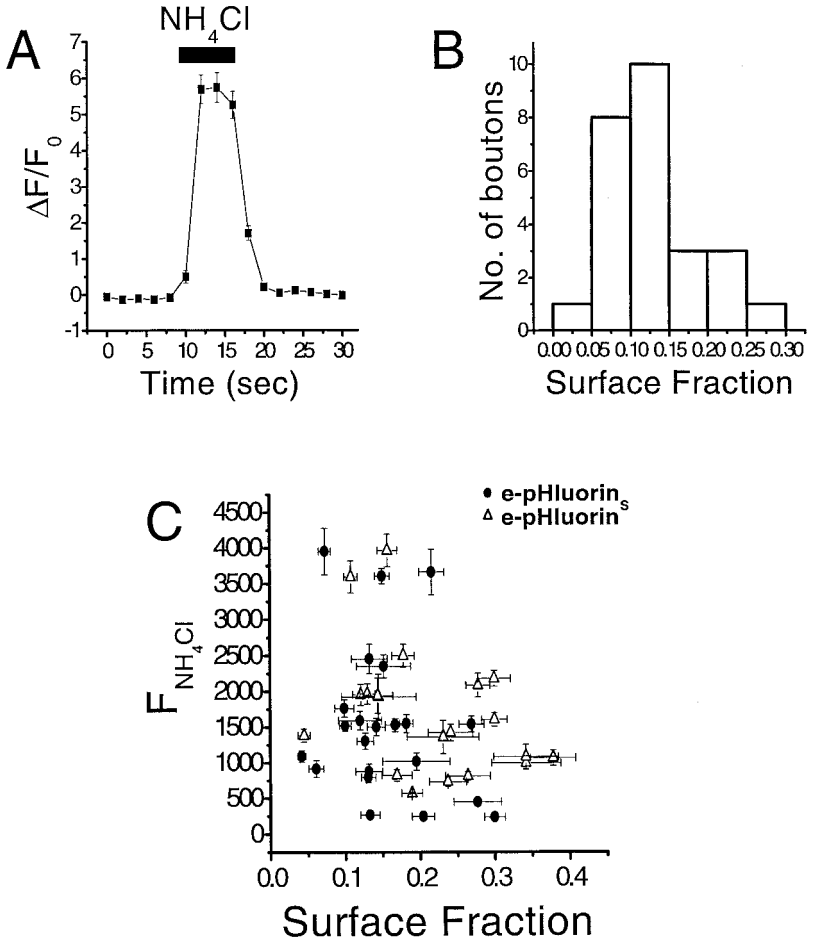

FIGURE 3 Estimates of surface expression of synapto-pHluorin at synaptic terminals. (*A*) The time course of average fluorescence intensity over 26 boutons during alkalization with ammonium chloride. The change in fluorescence (ΔF) normalized to initial fluorescence (F_0), obtained by averaging the first five data points, is plotted as a function of time. (*B*) The distribution of surface fraction of synapto-pHluorin from the same set of boutons as that shown in *A*. The surface fraction was calculated from the peak ammonium chloride response, $\Delta F/F_0$, using Eq. 7 (see text). Surface fraction (f) = $(\alpha - \gamma)/(\alpha\gamma + \alpha)$ where γ is the peak $\Delta F/F_0$ following NH_4Cl, and α is the relative change in fluorescence for pH change from 5.6 to 7.4 for probe with pK of 7.1. (*C*) Surface fraction is only weakly (inversely) correlated with expression levels of synapto-pHluorin (correlation coefficient = −0.39 and −0.22). Estimates of the expression level of synapto-pHluorin was obtained by measuring the average peak fluorescence signal in the presence of NH_4Cl (F_{NH_4Cl}) and plotted against the average surface fraction derived from Eq. 7 for $n = 20$ (ecliptic) and $n = 22$ (supercliptic) experiments each comprising 20–30 synaptic boutons. The e-pHluorin and e-pHluorin$_s$ data were obtained using different sensitivity settings, and so the relative intensity cannot be compared in these experiments. The average surface fraction derived from e-pHluorin-expressing terminals was 0.21 ± 0.02 and from e-pHluorin$_s$-expressing terminals was 0.15 ± 0.01.

relationship between the total synapto-pHluorin content (F_{NH_4Cl}) and surface fraction, for pooled data from ecliptic and superecliptic pHluorin-expressing hippocampal cultures, from a total of 42 different experiments (each with 20–40 boutons). There was a narrow range of surface fraction values, from 0.04 to 0.3 with mean of 0.15 ± 0.01, a median of 0.13 and only a very weak inverse correlation between the total amount of synapto-pHluorin and the measured surface fraction.

Signals measured during action potential firing

We next compared the fluorescence signals obtained during action potential firing at synaptic terminals expressing either ecliptic synapto-pHluorin, or a VAMP-EGFP fusion construct. Figure 4 shows the time course of fluorescence changes averaged over a collection of individual synaptic boutons that were expressing either synapto-pHluorin or VAMP-EGFP during a train of 300 action potentials. In each case, action potential stimulation led to an increase of fluorescence intensity. Following the cessation of the stimulus, fluorescence intensities returned to baseline levels. These signals depend upon successful exocytosis (Miesenböck et al. 1998) and the kinetics of the recovery is limited primarily by the rate of endocytosis of VAMP from the presynaptic plasma membrane (Sankaranarayanan and Ryan, 2000). Although action potential-induced signals are detectable using EGFP, a much more robust signal is obtained using e-pHluorins. The signals obtained using synapto-pHluorin (expressed as $\Delta F/F_0$) were ~ 4–10-fold greater than those obtained with EGFP-based detection. For purposes of illustration, we have shown our best EGFP responses compared to a typical e-pHluorin response. It is important to note, however, that the exact magnitude of fluorescence responses varies from synapse to synapse for both EGFP- and pHluorin-based measurements. Typical average peak signals during sustained action potentials for synapto-pHluorin varied from 0.8 to 2, whereas those from EGFP-VAMP varied from 0.1 to 0.4. Part of this variation arises from differences in the ratio of the amount of surface VAMP to the size of the vesicular pool of VAMP.

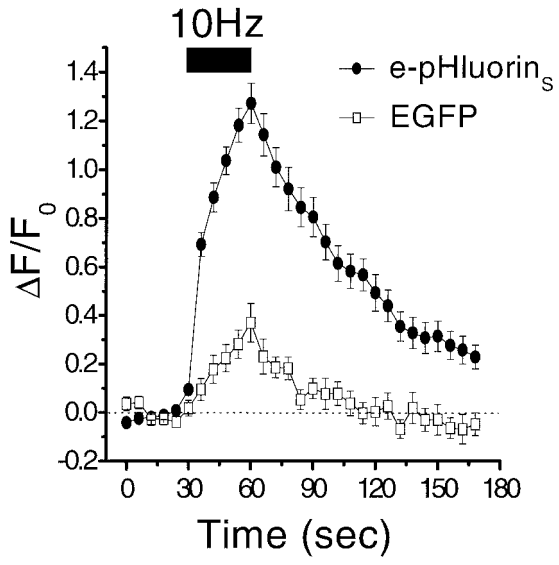

FIGURE 4 Fluorescence signals elicited during action potential firing from synapto-pHluorin (superecliptic) and VAMP-EGFP-expressing terminals. Time course of the average fluorescence response during a train of 300 action potentials at 10 Hz in hippocampal terminals expressing synapto-pHluorin (n = 21 boutons) and VAMP-EGFP (n = 20 boutons). The change in fluorescence (ΔF) normalized to initial fluorescence (F_0), average of the first five data points, is plotted as a function of time.

A quantitative relationship between the magnitude of $\Delta F/F_0$ measured during repetitive AP firing and the number of exocytosis events is easily derived. The magnitude of the signal ΔF (in photons collected per sample time) per synaptic vesicle undergoing exocytosis, i.e., experiencing a pH change from 5.6 to 7.4, is given by an expression similar to Eq. 2:

$$\Delta F = \left(\frac{1}{(1 + 10^{pK-7.4})} - \frac{1}{(1 + 10^{pK-5.6})}\right) * \beta * n_v, \qquad (9)$$

where β gives the number of detected photons per deprotonated e-pHluorin, and n_v is the number of e-pHluorins per vesicle. The term β reflects experimental instrumentation factors including illumination intensity, collection efficiency, and photochemical properties such as the extinction coefficient and quantum efficiency of the chromophore. The baseline signal F_0 arises from the fluorescence of pHluorins in a pool of N vesicles at pH 5.6 and the equivalent of $N * f/(1 - f)$ vesicles worth resident on the plasma membrane surface at pH 7.4 and is given by the expression

$$F_0 = \left(\frac{1}{(1 + 10^{pK-5.6})} + \frac{f}{(1-f) * (1 + 10^{pK-7.4})}\right) * \beta * N * n_v. \qquad (10)$$

Thus the fractional increase in fluorescence per synapse for each exocytosis event is given by

$$\frac{\Delta F}{F_0} = \frac{\left(\frac{1}{1 + 10^{pK-7.4}} - \frac{1}{1 + 10^{pK-5.6}}\right)}{\left(\frac{1}{1 + 10^{pK-5.6}} + \frac{f}{(1-f) \times (1 + 10^{pK-7.4})}\right)} \times \frac{1}{N} = \frac{\delta}{N}. \qquad (11)$$

This formula provides a quantitative means of calibrating pH-based optical measurements of exocytosis in terms of the fraction of the total acid synapto-pHluorin pool that is alkalinized. For a surface fraction f = 0.12, pK = 7.1, we obtain δ = 5.4. Thus, if there is a pool of ~100 acidic vesicles and in the absence of any endocytosis, each exocytosis event will give a relative fluorescence change of

5.4%. Measurements in the same system using EGFP (pK = 6.0) would yield $\delta = 1.65$. It is important to note that the dynamic measurements of fluorescence will represent a balance between the amount of exocytosis (as predicted by Eq. 11) and the amount of endocytosis over a given time period. Our previous measurements indicate that the initial rate of endocytosis is ~1 vesicle/sec, independent of the amount of exocytosis (Sankaranarayanan and Ryan, 2000), and thus Eq. 11 should provide a good estimate of the net signal for brief periods of AP firing.

What is the optimal pK for detection of presynaptic exo-endocytosis?

The sensitivity of optically based detection of presynaptic exocytosis is determined by a number of parameters. Ultimately, the total number of photons collected during synaptic activity determines the quality of the signal. Because most optical probes have finite photochemical lifetimes, only a limited number of photons can be detected before inducing either significant photodamage to the biological system or photobleaching of the reporter. An important question for future probe development is what is the ideal value of the pK for detecting exocytosis events using a pH-sensing strategy? Optimizing this parameter will then give the optimal signal for a given number of total collected photons. We have developed an analysis of this problem using a simple analytical framework. The sensitivity of measurements of presynaptic activity is determined by the relative size of ΔF compared to the magnitude of the fluctuations in the baseline signal. In general, the magnitude of the baseline signal fluctuations can be parameterized as the square root of the sum of the variances of all noise sources in the system. The standard deviation of the baseline signal, σ_T, is given by

$$\sigma_T = \sqrt{\sigma_{F_0}^2 + \sigma_I^2 + \sigma_x^2}, \tag{12}$$

where $\sigma_{F_0} = \sqrt{F_0}$ arises purely from photon-counting statistics of the fluorescence generated by the pHluorins (given by Eq. 10). σ_I ($= gF_0$), represents the noise arising from fluctuations (of magnitude $\sqrt{g}$) in the illumination intensity. σ_x^2 is the variance due to all other sources, such as dark current or other electronic noise. In general, the fluctuations in the illumination are only ~1–2% in magnitude, and are usually much smaller than the noise arising from photon-counting statistics (e.g., for photons/sample $< 10^4$).

To understand how the value of pK will contribute to the sensitivity of the detection, we provide a simple analysis of the signal to noise for this approach with regard to factors that depend upon pK. To gain a more intuitive insight into this problem, we have examined how ΔF, $\Delta F/F_0$, F_0, and $\Delta F/\sqrt{F_0}$ depend on the value of pK and f (the surface fraction) for a situation where the fluorophore makes a transition from pH of 5.6 to 7.4. We have assumed for now that measured baseline F_0 arises solely from pHluorin fluorescence as described in Eq. 10.

Figure 5 *A* shows a plot of $\Delta F/(\beta n_v)$ as a function of pK (derived from Eq. 9). The largest absolute change in signal occurs at a value of pK = 6.5, exactly in the middle of the change in pH 5.6–7.4. When the pK is much higher, the system effectively becomes insensitive to pH changes in the range of interest. Under experimental conditions however, one usually measures $\Delta F/F_0$. The dependence of $\Delta F/F_0$ on pK is shown in Fig. 5 *B* for a range of values of f (Eq. 11). The quantity displayed in Fig. 5 *B* is the product $\delta = N * \Delta F/F_0$ for a single exocytosis event. The predicted value of the observable quantity, $\Delta F/F_0$, is obtained by dividing δ by the number of pHluorin-labeled vesicles N in the synaptic terminal and multiplying by the total number of exocytosis events. Two important features can be seen in Fig. 5 *B*. First, the dependence of δ on pK shows a sigmoidal behavior. At low pK the predicted signal-to-background ratio is very small. This arises from the fact that, for pK values below the resting vesicle pH of 5.6, all of the fluorescent reporter molecules will already be deprotonated, so a shift to pH 7.4 will not generate a signal. At very high values of pK, the predicted $\Delta F/F_0$ reaches a plateau. This behavior can be understood by analyzing the magnitude of the baseline signal F_0 along with ΔF as a function of pK. At high values of pK (> 8), F_0 becomes very small, but so does the predicted size of ΔF for a pH change from 5.6 to 7.4. Figure 5 *C* shows a plot of the quantity $F_0/(N\beta n_v)$, (derived from Eq. 10) as a function of the pK. The plateau phase in $\Delta F/F_0$ therefore arises from the parallel drop in F_0 and ΔF for pK values above 8. Although the curves in Fig. 5 *C* suggest that the optimal pK would be >8, one must also consider that both the baseline and signal sizes become very small in this range.

In an ideal optical-based detection scheme, the baseline signal fluctuations will arise solely from photon-counting statistics where $\sigma_T = \sqrt{F_0}$. The signal-to-noise ratio (s/n) for this case is given by

$$\frac{s}{n} = \frac{\Delta F}{\sqrt{F_0}} = \sqrt{\frac{\beta n_v}{N}} \times \frac{1/[(1 + 10^{pK-7.4}) - (1 + 10^{pK-5.6})]}{\sqrt{[1/(1 + 10^{pK-5.6})] + [f/(1 - f) * (1 + 10^{pK-7.4})]}}. \tag{13}$$

The signal-to-noise ratio for detecting multiple exocytosis events at the same synaptic terminal will increase in proportion to the number of events. Inspection of Eq. 13 indicates that, in addition to the total number of photons collected (which is proportional to the number of pHluorin molecules), the sensitivity of pH-based detection of presynaptic activity is governed by the pK for protonation, the fractional surface expression of the reporter, and the total size of the labeled synaptic vesicle pool. The optimal value

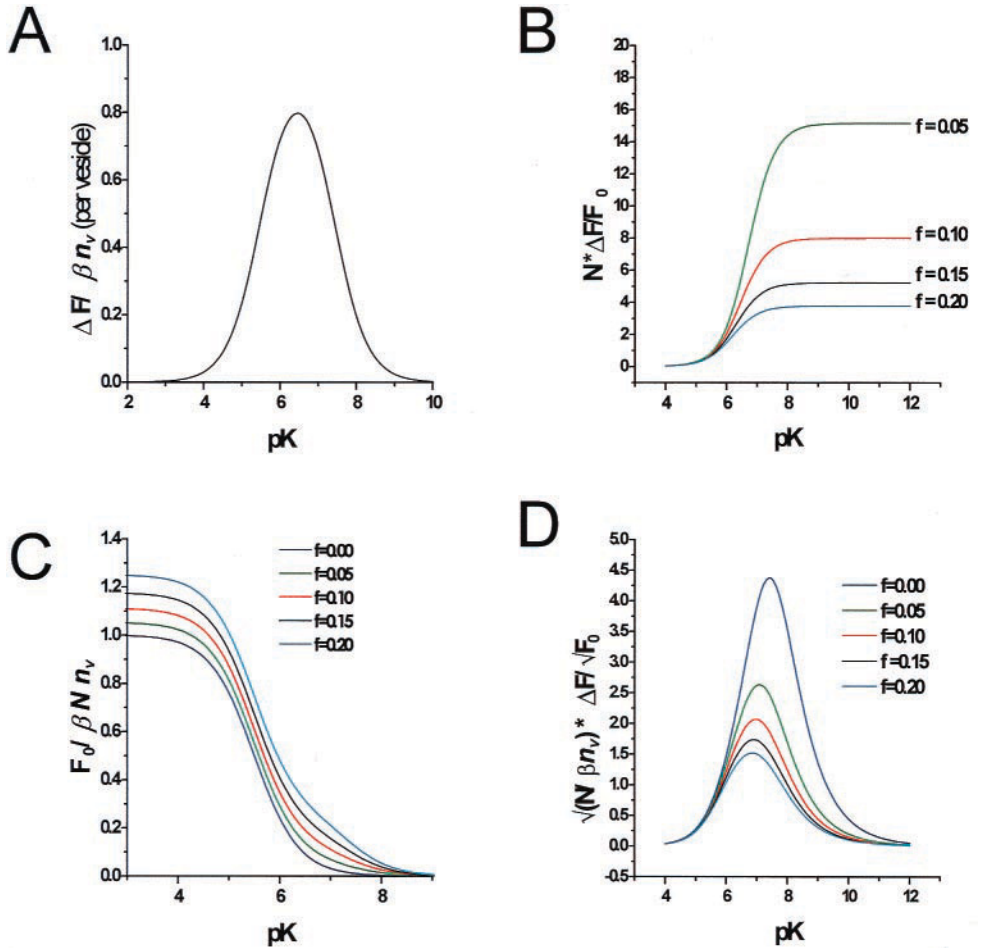

FIGURE 5 Calculation of the relationship between experimentally measured optical parameters as a function of pK and surface fraction for a fluorophore that undergoes a pH change from 5.6 to 7.4. The relationship between (*A*) change in fluorescence (ΔF); (*B*) change in fluorescence relative to initial fluorescence ($\Delta F/F_0$); (*C*) initial fluorescence (F_0); and (*D*) The signal-to-noise ratio ($\Delta F/\sqrt{F_0}$) and pK of fluorophore are illustrated. The surface fractions *f*' are denoted by the different colors in *B*, *C*, and *D*. The equations used to obtain the curves are Eqs. 9, 11, 10, and 12 described in the text.

of pK with respect to the sensitivity of detection of exocytosis is obtained by maximizing the value of the second factor in Eq. 13, i.e., where

$$\frac{\partial}{\partial pK}\frac{\Delta F}{\sqrt{F_0}} = 0. \qquad (14)$$

Figure 5 *D* shows a plot of the expected signal-to-noise ratio as a function of pK for a range of values of *f*. Here, a single absolute maximum in the signal-to-noise ratio is apparent. This optimal value is easily determined graphically, and varies slightly depending on the surface expression levels. For $f = 0.12$, the average measured value in our experiments, the optimal pK is ~7.2. Thus, in terms of signal-to-noise considerations, the randomly selected mutations in ecliptic pHluorin resulted in the generation of a protein with an almost ideal pK (~7.1, see Fig. 2 *C*) for detecting exocytosis of synaptic vesicles in a detection system where the noise is dominated by photon-counting statistics. For cases where the shot noise of collected photons does not dominate, the ideal pK will shift closer to the value of pK that maximizes ΔF, i.e., pK = 6.5 (Fig. 5 *A*). This arises because the term in the denominator of the signal-to-noise ratio will be dominated by factors that do not depend upon pK.

DISCUSSION

The advent of genetically encoded reporters has revolutionized the types of biological signals that can be tracked in living systems. To understand these signals quantitatively, it is important to establish the physical–chemical framework of their origin. Here, we have examined the properties and the theoretical basis of novel indicators of presynaptic exocytosis that report pH of their environment. Our analysis indicates that ecliptic pHluorins are well suited for measuring AP-driven exocytosis, but that the sensitivity will ultimately be governed by a number of cell biological constraints.

Ecliptic pHluorin behaves as an all-or-none pH-dependent fluorescence indicator

Analysis of the pH dependence of e-pHluorin fluorescence indicates that the system is well described by a simple equilibrium between a nonfluorescent protonated state and a fluorescent deprotonated state (described by Eq. 1). This is similar to the behavior of EGFP, the commonly used "enhanced" variant of wild type GFP, and is consistent with the original description of this new variant of GFP (Miesenböck et al., 1998). As a result, the magnitude of signals generated upon pH changes from 5.6 to 7.4 will be determined by the fraction of molecules in the deprotonated state at each of these pH values. Thus, even though the fluorescence undergoes all-or-none switching at the individual molecule level, the net fluorescence will be determined by equilibrium values of proton binding, and hence the value of the pK. The data in Fig. 3 indicate that e-pHluorins have a pK of 7.1, and thus the increase in fluorescence for each vesicle fusing with the plasma membrane will be ~20-fold.

Surface expression of synapto-pHluorin increases the background level

Although the shift in the apparent pK of e-pHluorin compared to EGFP makes e-pHluorin nearly optimal for this application, the actual magnitude of the signals compared to background levels are constrained by a number of cellular properties. One unexpected but important contribution to the background signal is the appearance of a small fraction of the synapto-pHluorin on the external membrane of the cell. Although the surface fraction is relatively small at presynaptic terminals (~0.04–0.3), these molecules will be, on average, ~20-fold more fluorescent than the synapto-pHluorins localized within acidic organelles. The origin of this surface population of VAMP remains unclear. It may simply arise from small inefficiencies in the recycling process of synaptic vesicles or result from an alternate membrane trafficking pathway. It has previously been reported that synaptic plasma membrane-associated proteins such as syntaxin-1 and 25 Kd synaptosomal associated protein (SNAP-25) have been observed on synaptic vesicles, thus the apparent mislocalization of VAMP at the surface could, in fact, be physiologically relevant for synaptic function (Walch-Solimena et al., 1995). Further, we have observed that the degree of surface expression of pHluorins was not correlated with the total synapto-pHluorin content, suggesting that the surface distribution of pHluorins is not the result of overexpression in our transient expression system. It will be interesting in the future to determine whether the ratio of surface to vesicle concentration is a common feature of all synaptic vesicle membrane proteins. If the resting surface concentration can be reduced to zero, the signal-to-noise ratio for detecting exocytosis would increase by a factor of ~2 (compare the peak of the s/n curve in Fig. 5 D at $f = 0$ and $f =$ 0.15), and the signal-to-background ratio would increase ~4–5-fold in magnitude.

Finally a second constraint that affects the magnitude of AP-induced signals relative to background is the size of the vesicle pool (N). Synapses with larger vesicle pools will have larger background signals. The absolute sensitivity for detecting a specific number of exocytotic events will decrease in proportion to $1/\sqrt{N}$.

CONCLUSION

We have developed the formalism required to calibrate pH-based measurements of synaptic activity in terms of the fraction of the acidic pool of vesicles that undergoes exocytosis during action potential firing. One must also consider that the signals are only transient in nature, and reequilibrate to baseline via a sequence of endocytic and reacidification steps. The absolute magnitude of the signals will thus represent a balance at any given time between the kinetics of exocytosis and endocytosis, similar to electrical measurements of membrane capacitance. The framework and methodologies developed here should prove useful for future applications of this technology for dissection of synaptic vesicle-recycling events and for measurements of synaptic activity in intact or semi-intact neural networks. Further, this analytical framework should aid in the development of alternative color variants of GFP such as the red-shifted, coral reef-derived fluorescent proteins (Matz et al., 1999) for pH-sensitive applications.

We would like to thank Dr. Watt Webb for useful discussions, Wayne Yan for excellent technical assistance, and Dr. Richard Scheller (Stanford University) for providing the VAMP-EGFP construct. The National Institutes of Health grant NS24692 (T.A.R) supported this work. T.A.R. is an Alfred P. Sloan Research fellow. The development of the enhanced ecliptic probe was supported by the Mathers Foundation (J.E.R).

REFERENCES

Denk, W., and K. Svoboda. 1997. Photon upmanship: why multiphoton imaging is more than a gimmick. *Neuron.* 18:351–357.

Haupts, U., S. Maiti, P. Schwille, and W. W. Webb. 1998. Dynamics of fluorescence fluctuations in green fluorescent protein observed by fluorescence correlation spectroscopy. *Proc. Natl. Acad. Sci. USA.* 95: 13573–13578.

Helmchen, F., K. Svoboda, W. Denk, and D. W. Tank. 1999. In vivo dendritic calcium dynamics in deep-layer cortical pyramidal neurons. *Nat. Neurosci.* 2:989–996.

Kneen, M., J. Farinas, Y. Li, and A. S. Verkman. 1998. Green fluorescent protein as a noninvasive intracellular pH indicator. *Biophys. J.* 74: 1591–1599.

Liu, Y., Krantz, D. E., Waites, C., and R. H. Edwards. 1999. Membrane trafficking of neurotransmitter transporters in the regulation of synaptic transmission. *Trends Cell Biol.* 9:356–363.

Matz, M. V., A. F. Fradkov, Y. A. Labas, A. P. Savitsky, A. G. Zaraisky, M. L. Markelov, and S. A. Lukyanov. 1999. Fluorescent proteins from nonbioluminescent Anthozoa species. *Nature Biotech.* 17:969–973.

Miesenböck, G., D. A. De Angelis, and J. E. Rothman. 1998. Visualizing secretion and synaptic transmission with pH-sensitive green fluorescent proteins. *Nature.* 394:192–195.

Nelson, N. 1992. Structure and function of V-ATPases in endocytic and secretory organelles. *J. Exp. Biol.* 172:149–153.

Roos, A., and W. F. Boron. 1981. Intracellular pH. *Physiol. Rev.* 61: 296–434.

Ryan, T. A. 1999. Inhibitors of myosin light chain kinase block synaptic vesicle pool mobilization during action potential firing. *J. Neurosci.* 19:1317–1323.

Sankaranarayanan, S., and T. A. Ryan. 2000. Real-time measurements of vesicle-SNARE recycling in synapses of the central nervous system. *Nature Cell Biol.* 2:197–204.

Schikorski, T., and C. F. Stevens. 1997. Quantitative ultrastructural analysis of hippocampal excitatory synapses. *J. Neurosci.* 17:5858–5867.

Threadgill, R., K. Bobb, and A. Ghosh. 1997. Regulation of dendritic growth and remodeling by Rho, Rac, and Cdc42. *Neuron.* 19:625–634.

Tsien, R. Y. 1998. The green fluorescent protein. *Annu. Rev. Biochem.* 67:509–544.

Walch-Solimena, C., J. Blasi, L. Edelmann, E. R. Chapman, G. F. von Mollard, and R. Jahn. 1995. The t-SNAREs syntaxin-1 and SNAP-25 are present on organelles that participate in synaptic vesicle recycling. *J. Cell Biol.* 128:637–645.